Electronic Supplementary Information (ESI) for RSC Advances.
This journal is © The Royal Society of Chemistry 2022

Electronic supplementary information (ESI)

Waterborne superamphiphobic coatings with network structure for enhancing mechanical durability

Wancheng Gu, Wei Wang, Xuan Jiao, Weilin Deng, Yage Xia, Xinquan Yu, Youfa Zhang*

Jiangsu Key Laboratory of Advanced Metallic Materials, School of Materials Science and Engineering, Southeast University, Nanjing 211189, P. R. China.

*Corresponding author: yfzhang@seu.edu.cn

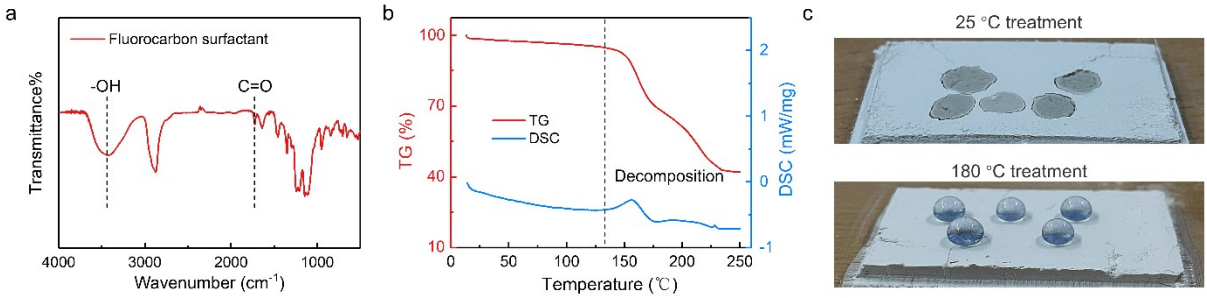

Fig. S1. Wettability control of fluorinated nano-silica. (a) Fourier transform infrared (FTIR) spectra of fluorocarbon surfactant. The carboxyl groups (-COOH) on fluorocarbon surfactant make fluorinated nano-silica hydrophilic. (b) Thermogravimetric analysis (TG) of fluorocarbon surfactant showing the decomposition temperature. (c) Optical photographs showing the wettability difference of fluorinated nano-silica treated at 25 °C and 180 °C for 10 min. The superamphiphobicity is improved gradually with the decomposition of fluorocarbon surfactant (i.e., treatment temperature).

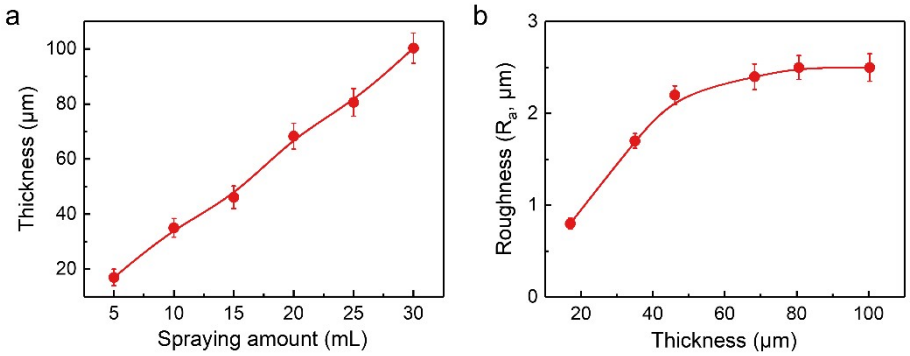

Fig. S2. Influence of the coating thickness on the surface roughness of the network coatings. (a) Change of the coating thickness along with the spraying amount of the coating suspension. (b) Change of the surface roughness as a function of the coating thickness. The thickness of network coatings can be increased by increasing the spraying amount of the coating suspension, which improves the crosslinking of the network structure. Therefore, the coating roughness increases at first and then becomes stable when the thickness reaches ~45 μm, indicating the network structure formation.

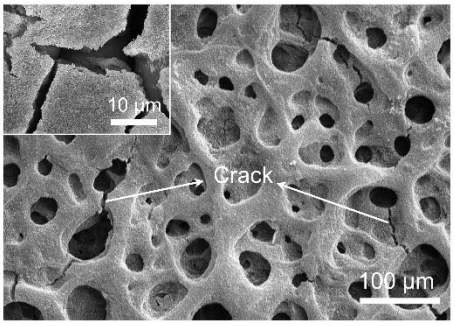

Fig. S3. Influence of the coating treatment temperature on the network structure. Surface morphology of the network coating treated at 200 °C. Increasing the treatment temperature to more than 180 °C results in the crack formation on the network structure, which weakens the coating mechanical stability.

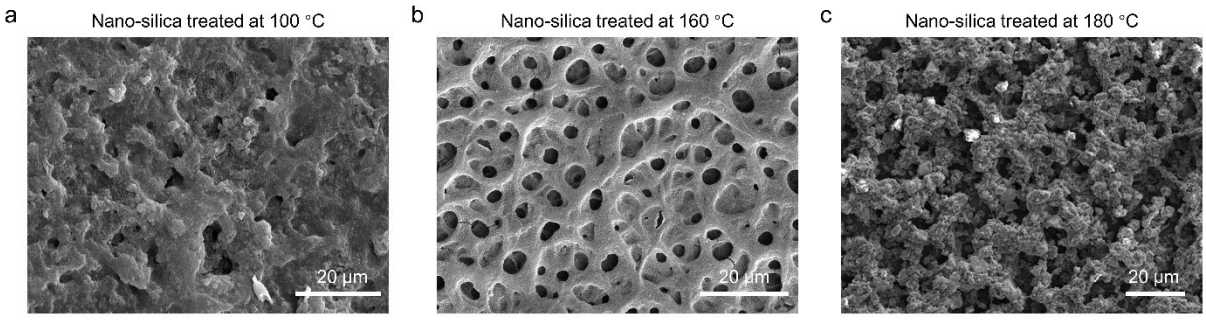

Fig. S4. Network structure control by tailoring the wettability of fluorinated nano-silica. Surface morphologies of network coatings prepared by using the fluorinated nano-silica treated at (a) 100 °C, (b) 160 °C, and (c) 180 °C for 10 min, respectively.

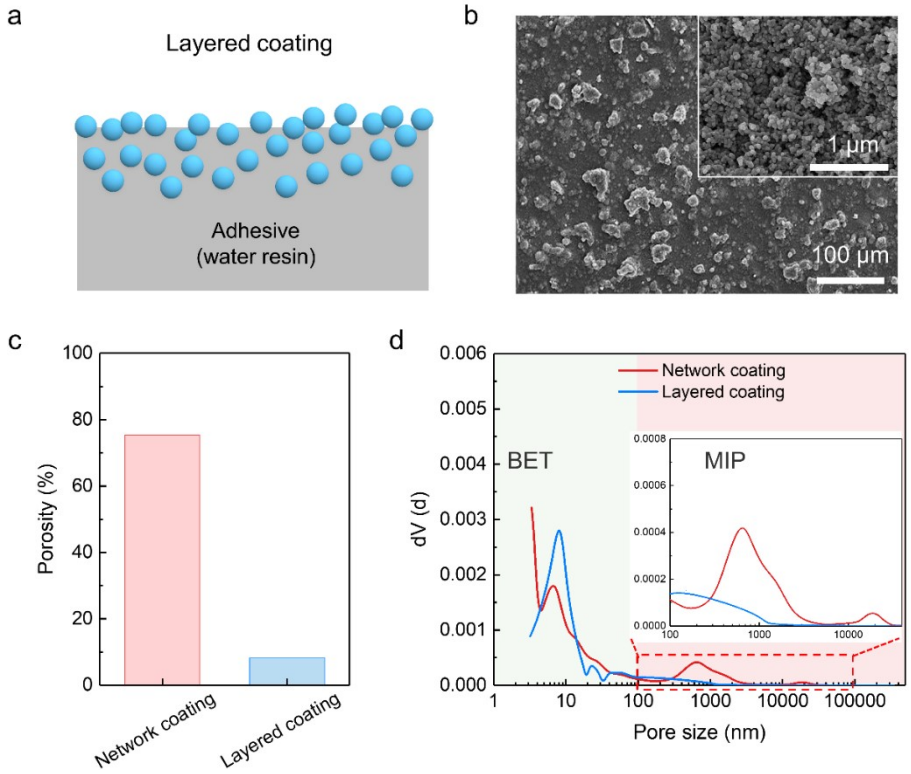

Fig. S5. The structure comparison between the network coating and layered coating. (a) Schematic illustration of the layered coating. (b) Surface morphology of the layered coating. (c) The porosity of the network coating and layered coating. (d) The distributions of pore size of the network coating and layered coating. Due to the network structure, our coating possesses much more pores than the layered coating, especially the micro-scale ones.

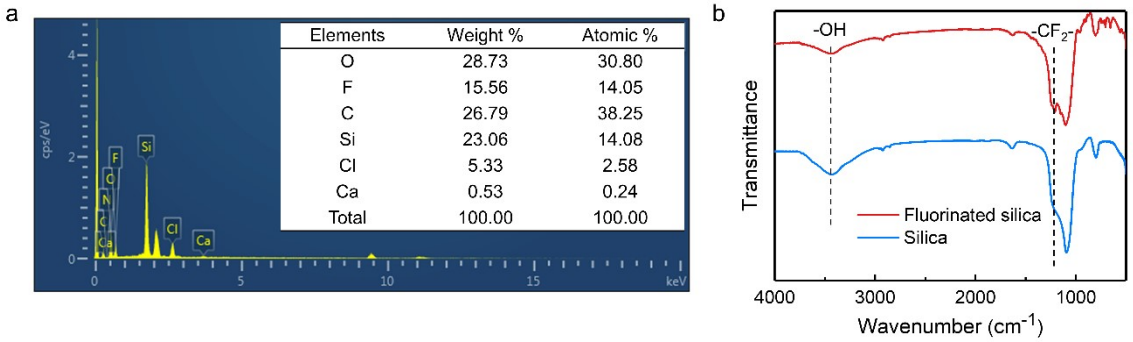

Fig. S6. The demonstration of nano-silica fluorination. (a) EDS spectra of the network coating. (b) FTIR spectra of nano-silica before and after fluorination. The fluorinated silica was treated at 180 °C for 10 min before the measurement. The weaker peak of -OH groups and a new peak of -CF_2- groups on nano-silica demonstrate the successful graft of FDTS.

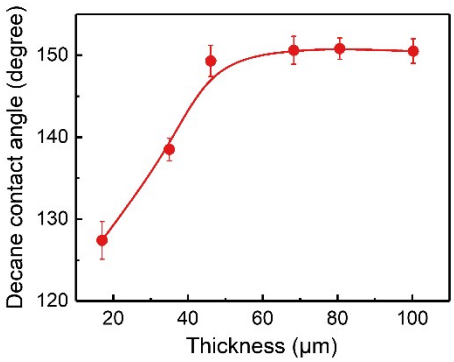

Fig. S7. Influence of the thickness of network coatings on the superamphiphobicity. Change of decane contact angles as a function of the coating thickness. To highlight the influence of the coating thickness on the superamphiphobicity, decane with low surface tension (23.8 mN/m) was chosen to assess the superamphiphobicity. Decane contact angles increase at first and then reach a platform, as the coating thickness increases. The network coating achieves excellent superamphiphobicity when the coating thickness is greater than ~45 μm. This is because the coating roughness increases with the thickness increment and then turns stable as mentioned in Fig. S2b.

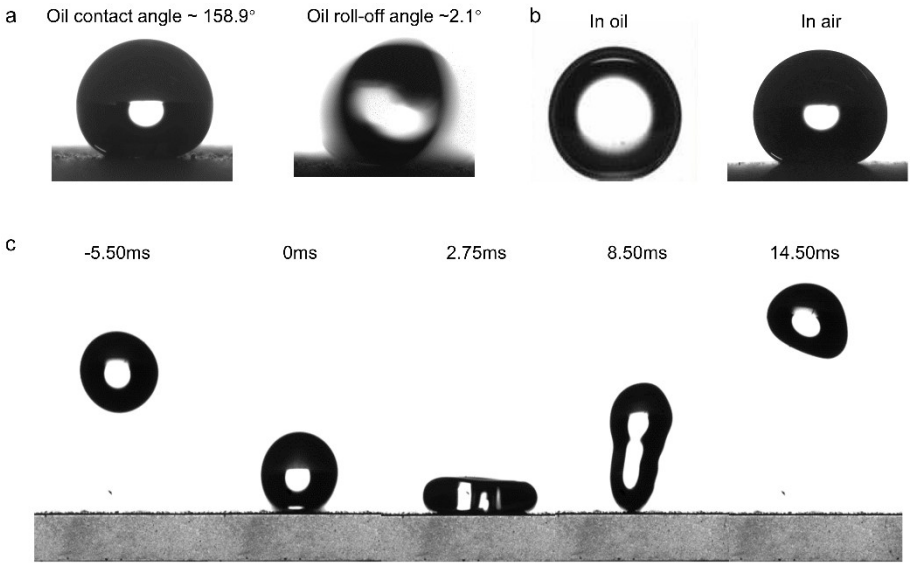

Fig. S8. The super-repellence to liquids of the network coating. (a) The super-repellence to olive oil. (b) The superhydrophobicity in olive oil and air. (c) The bounce procedure of decane droplet on the network coating.

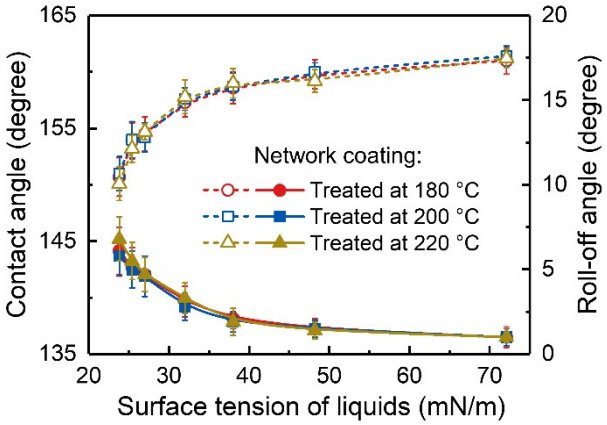

Fig. S9. Comparison of the superamphiphobicity of network coatings treated at different temperatures. Contact angles and roll-off angles of liquids with various surface tensions on network coatings treated at different temperatures. When the coating treatment temperature reaches 180 °C to remove the influence of the fluorocarbon surfactant on the superamphiphobicity, the contact angles and roll-off angles of various liquids on network coatings treated at 180 °C and higher temperatures (i.e., 200 °C and 220 °C) are similar, respectively.

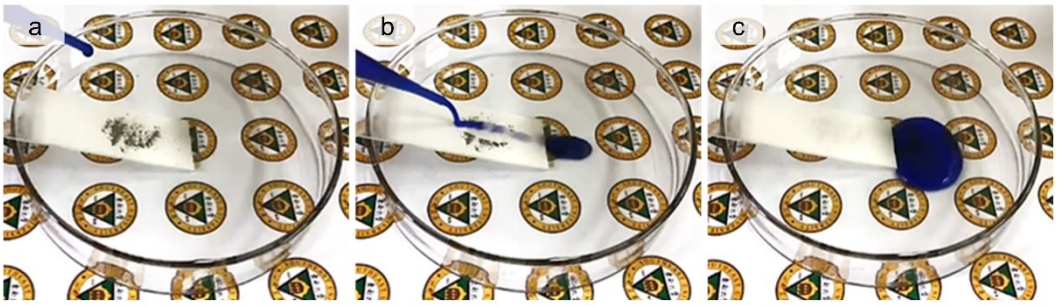

Fig. S10. Self-cleaning performance. (a) The dust on the coating surface. (b) The removal of dust by the ethanol solution (60 wt.%) flow. (c) The clean coating surface.

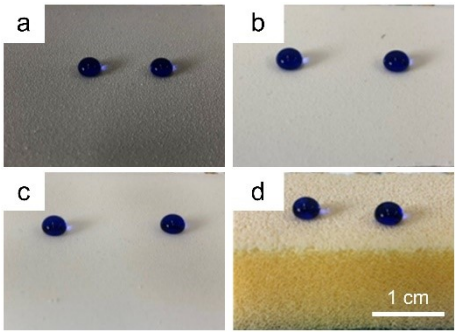

Fig. S11. The versatility of the network coating. Optical photographs of application to various substrates, including (a) tinplate, (b) polypropylene, (c) paper, and (d) sponge.

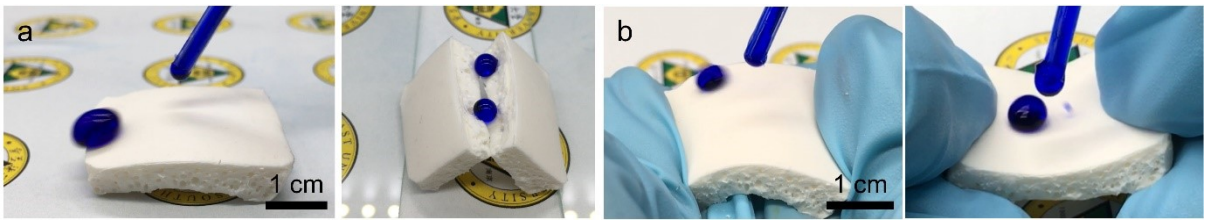

Fig. S12. Network bulk. (a) The superamphiphobicity of the upper and inner surface. (b) The droplet of ethanol solution (60 wt. %) with spherical shape on the bent bulk.

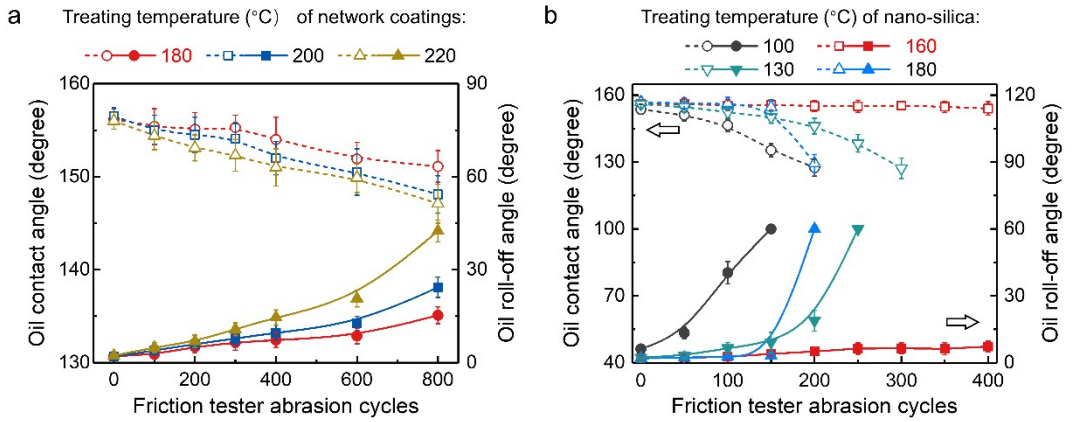

Fig. S13. The influence of the network structure on mechanical durability. (a) Contact angles and roll-off angles of olive oil on the abraded network coating treated at different temperatures. (b) Contact angles and roll-off angles of olive oil on the abraded network coating with fluorinated nano-silica treated at different temperatures.

Note

As mentioned in Fig. S3, treatment temperature higher than 180 °C results in the crack formation on the network structure. The network structure becomes fragile under mechanical abrasion, leading to the deterioration of the protection capacity. Therefore, the network coating treated at 200 °C shows a faster deterioration of superamphiphobicity than the network coating treated at 180 °C (Fig. S13a). Such a tendency is more obvious when further increasing the treatment temperature (i.e., 220 °C). Considering both superamphiphobicity and durability, 180 °C is the optimum temperature.

Similarly, the network structure influenced by fluorinated nano-silica treated at different temperatures also shows an impact on the mechanical durability (Fig. S4). With the network structure for protection, the network coating with fluorinated nano-silica treated at 160 °C shows the best abrasion resistance (Fig. S13b).

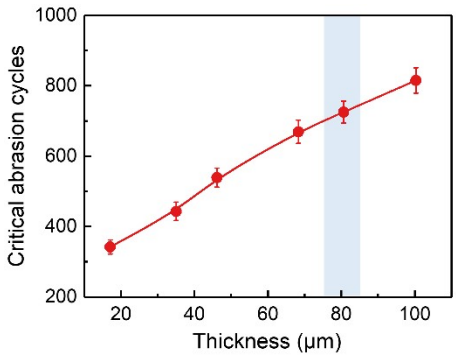

Fig. S14. Influence of the coating thickness on the abrasion resistance of network coatings. Change of critical abrasion cycles as a function of the coating thickness. It is well known that coating durability relates to the coating thickness. The critical abrasion cycles increase with the increment in coating thickness. Therefore, the coating thickness can be adjusted according to the requirement of durability, when larger than 45 μm for achieving superamphiphobicity. From an engineering perspective, a relatively thin coating with a thickness of ~80 μm is recommended, which achieves both satisfactory superamphiphobicity and durability.

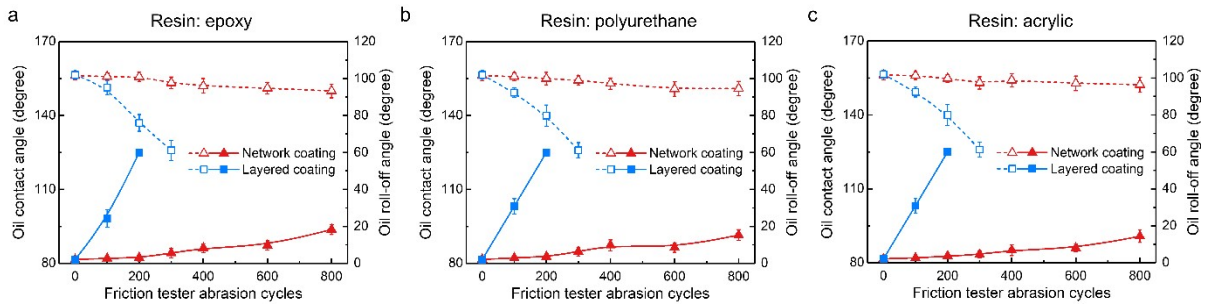

Fig. S15. The universality of the network coating for dramatically enhancing the mechanical durability. Contact angles and roll-off angles of olive oil on the abraded network coating prepared by waterborne (a) epoxy, (b) polyurethane, and (c) acrylic resin.

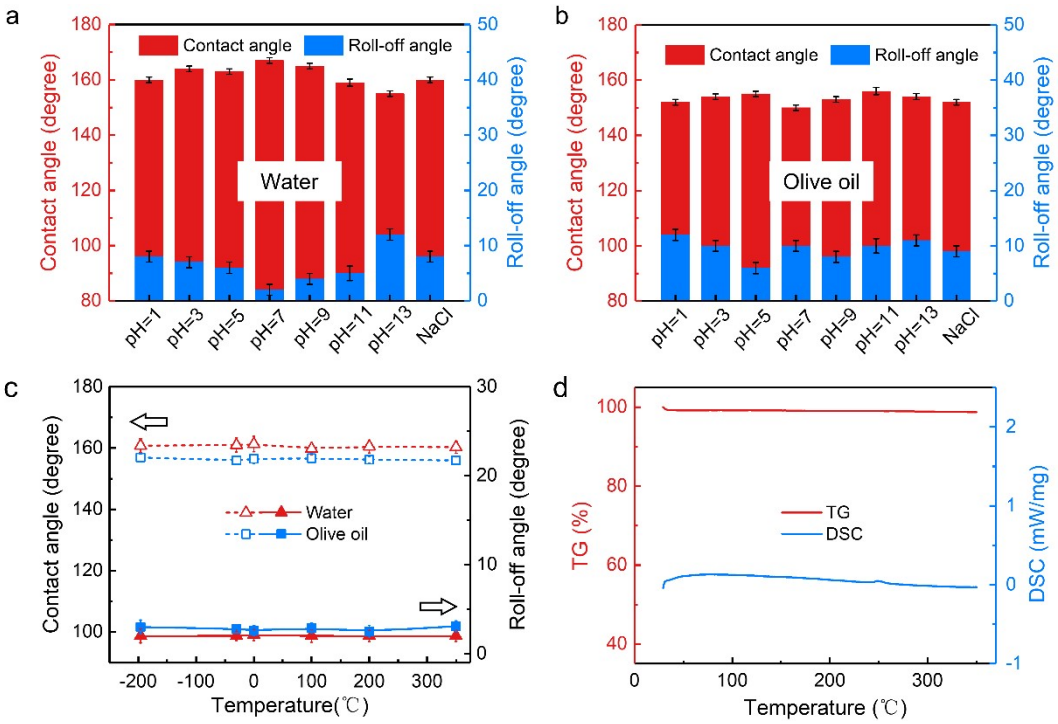

Fig. S16. Chemical and thermal stability of the network coating. The (a) water and (b) olive-oil repellence of network coating after immersion in different corrosive solutions (pH value ranging from 1-13) for 48 h. (c) Superamphiphobicity of the coating after treatment at a temperature ranging from -196 to 350 °C. The treatment time at each temperature point is 2 h. (d) Thermogravimetric analysis of the network coating. The weight loss is negligible during the heating procedure, showing excellent thermal stability.

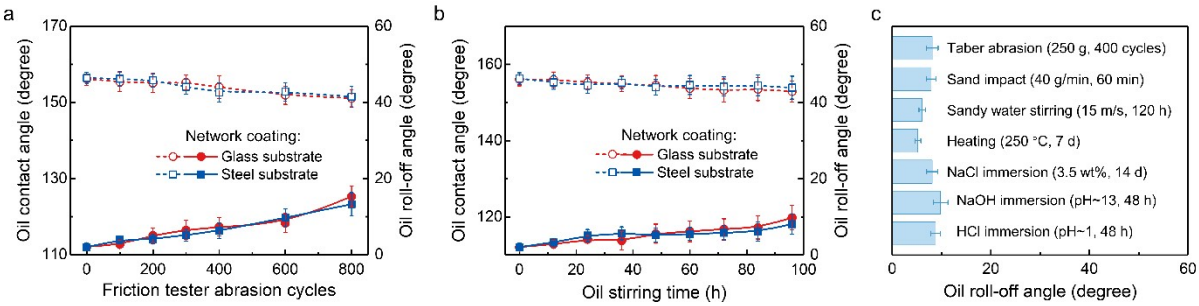

Fig. S17. Comprehensive durability of network coatings on the steel substrate. (a, b) Olive-oil repellence of network coatings on different substrates after friction tester abrasion and oil stirring, respectively. (c) Comprehensive durability of network coatings on the steel substrate. These tests were the same as those performed on network coatings on the glass substrate. The network coatings on the steel substrate show similar durability to those on the glass substrate.

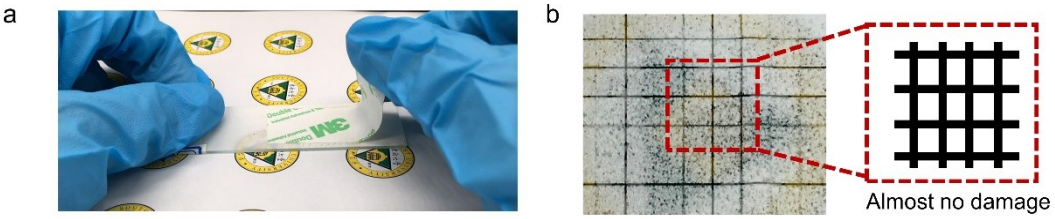

Fig. S18. The substrate adhesion of the network coating. (a) Tape peeling test after crosshatching according to the ASTM D3359-17 standard. (b) Optical photograph showing the strong adhesion of the network coating.

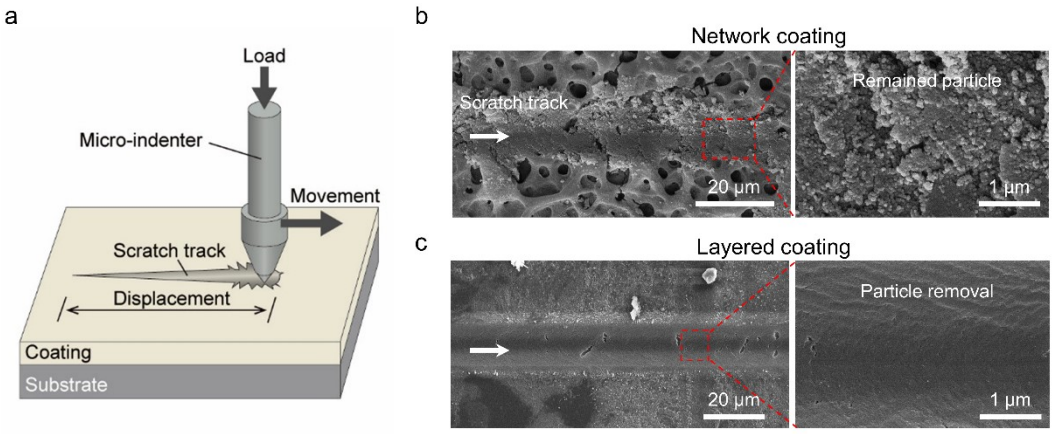

Fig. S19. Mechanical stability of the network coating. (a) Schematic showing the micro-scratching test. SEM images of (b) network coating and (c) layered coating after micro-scratching under the load of 10 mN. For the micro-scratching test, the sample was loaded on an instrument (Nano Test Vantage, Micro Materials Corporation) with a diamond indenter (tip size: 5 μm), and the indenter scratched over the samples at a velocity of 5 μm/s under a normal load. The scratch morphology under 10-mN load was characterized for the anti-abrasion evaluation.

Table S1. Surface tension of the tested liquids

Name	Surface Tension (mN/m)	Name	Surface Tension (mN/m)
Water	72.1	Ethylene glycol	48.2
Formic acid	38	Olive oil	32
Hexadecane	27	60 wt. % ethanol solution	25.4
Decane	23.8	-	-

Table S2. Network coatings prepared by various waterborne resins

Samples	FEVE		Epoxy		Polyurethane		Acrylic	
	Resin	Coating	Resin	Coating	Resin	Coating	Resin	Coating
Water contact angle	101.2	161.4	34.7	161.2	58.1	161.4	41.1	161.3
Oil contact angle	62.3	158.9	15.8	157.5	36.5	157.9	26.1	158